Variation of Distortion within the Photographic Field

Clive S. Fraser
Geodetic Services, Inc., 1511 South Riverview Drive, Melbourne, FL 32901
Mark R. Shortis
Department of Surveying and Land Information, University of Melbourne, Parkville 3052, Australia

ABSTRACT: For the attainment of the highest accuracies in close-range industrial photogrammetry, it is necessary to account for the variation of radial distortion within the photographic field, especially for large-format lenses. In this paper an empirical correction model is introduced which overcomes serious shortcomings in the traditionally applied geometric correction approach. The new model has been tested with success on a number of medium- and wide-angle, medium- and large-format lenses. The results of sample tests are presented, and the effectiveness and practicability of the empirical approach are discussed.

INTRODUCTION

THE PURSUIT OF OPTIMAL ACCURACIES in close-range photogrammetric triangulation makes it mandatory that the variation of lens distortion with object distance be compensated. Both radial and decentering distortion vary in a predictable manner with lens focusing (Brown, 1971; Brown, 1972; Fryer and Brown, 1986), with the strongest variation occurring at larger image scales. Typically less pronounced, though often still of significance, is the variation of radial distortion within the photographic field.

In Brown (1971, 1972) an expression is derived to account for changes in distortion between points on the plane of sharpest focus and object points at different distances from the camera :

$$\delta r_{ss'} = \frac{1}{\gamma_{ss'}} \delta r_{s'} \tag{1}$$

In essence, Equation 1 states simply that the radial distortion $\delta r_{ss'}$ at object distance s' for a lens focused at object distance s is proportional to the corresponding distortion value $\delta r_{s'}$ for the lens focused on an object plane at distance s'. The factor $\gamma_{ss'}$ is given as the ratio between the corresponding principal distances c_s and $c_{s'}$ for focused distances of s and s' (Brown, 1971):

$$\gamma_{ss'} = \frac{c_{s'}}{c_s} = \frac{s'}{s} \cdot \frac{(s - f)}{(s' - f)} \tag{2}$$

where f is the focal length of the lens. It should be noted that the parameter $\gamma_{ss'}$ is derived purely as a function of imaging geometry; Equation 2 contains no terms to account for the gradient of distortion variation with focused distance. Nevertheless, Brown showed experimentally that Equation 1 could be applied to a lens of moderate distortion gradient. He also noted that lens-to-lens variations in distortion performance can be significant for the same lens type.

Over the past half decade or so developments in close-range photogrammetric systems have led to the routine attainment of what were hitherto unheard of triangulation accuracies. Notable innovations in this regard have been the CRC cameras and submicrometer AutoSet monocomparator of Geodetic Services, Inc (GSI) STARS system (Fraser and Brown, 1986). In industrial photogrammetry it is nowadays not unusual to realize object point triangulation accuracies surpassing 1:400,000 of the size of the object when utilizing STARS. Corresponding closures of triangulation (RMS value of image coordinate residuals) of between 0.4 and 1.0 micrometres are typical.

With the capability both to measure film to sub-micrometre accuracies and model the projective equations of the self-calibrating bundle adjustment to such high resolution, it is possible to re-examine the validity and rigor of accepted mathematical models for lens distortion variation. Recent experience by the authors in this regard has led to the conclusion that the expression, Equation 1, for the variation of lens distortion within the photographic field is not universally valid. The factor $\gamma_{ss'}$ appears to consistently lead to an underestimation of the magnitude of the variation and does not correctly account for changes in the algebraic sign of distortion values.

As is often the case, the finding of a shortcoming in one mathematical model leads inexorably to the quest for alternative formulations. From the standpoint of mathematical rigor at least we have not been too successful in this quest. Promising leads were often frustrated when it was found not only that experimental results were not consistent with predictions, but also that results showed variations in distortion behavior between lenses of the same make and type. As an alternative to the theoretical, an empirical approach was adopted in the hope that some more insight could be gained into the problem. What eventually came about was a reasonably satisfactory and straightforward model which accounts for the variation of radial lens distortion within the photographic field. In the following sections of this paper the empirical model will be described, and experimental data which illustrates the effectiveness of this approach will be presented.

DISTORTION VARIATION FOR FIVE LENSES

To illustrate the variation of distortion within the photographic field, we will consider five example lenses. The first

TABLE 1. RADIAL LENS DISTORTION AT FOUR OBJECT PLANES FOR THE PENTAX 645VL CAMERA WITH 45-MM F/2.8 LENS. THE LENS IS FIXED-FOCUSED AT 8 METRES. UNITS ARE MICROMETRES.

Radial Distance (mm)	Object distance to plane (m) 1.5	2.1	2.6	3.4
4	2.4	2.5	2.4	2.4
8	18.7	19.0	18.8	18.8
12	59.3	60.1	59.7	59.6
16	128.5	129.5	128.7	128.5
20	219.9	220.5	219.2	218.8
24	313.1	312.9	310.5	309.5
28	368.8	369.5	364.1	362.3

PHOTOGRAMMETRIC ENGINEERING & REMOTE SENSING,
Vol. 58, No. 6, June 1992, pp. 851–855.

0099-1112/92/5806–851$03.00/0

camera is a Pentax PAMS645-VL with a 45-mm *f*/2.8 lens. Table 1 lists the Gaussian radial distortion for this lens for four planes within the photographic field: object distances of 1.5, 2.1, 2.6, and 3.4 metres. The corresponding image scales for the 45-mm lens which was focused at 8m (175×) are approximately 33×, 45×, 56×, and 75×, respectively. The four distortion profiles were determined from analytical plumbline calibrations (e.g., Fryer and Brown, 1986), with each data set comprising two photographs and close to 1000 plumbline observations. Image coordinate observations for this and the other plumbline calibrations reported were made on the AutoSet automatic monocomparator. An indication of the quality of this lens calibration process is given by the RMS value of image coordinate residuals, which for the Pentax averaged 1.7 micrometres.

A striking feature exhibited in Table 1 is the very small variation of distortion within the photographic field. It is only towards the edge and corners of the image format that we see a variation exceeding a few micrometres. Because there was neither a profile determined for the plane of best focus at 8 metres (the plumbline range was too small to fill the film format at this photographic scale) nor a profile measured for a second object distance (the lens is fixed focus), it was not possible to assess the validity of Equation 1 for this lens. Given the virtually zero gradient of distortion within the photographic field, however, it does seem likely that the $\gamma_{ss'}$ correction factor would be invalid in this case, unless, of course, if $\delta r_{s'}$ varied in direct proportion to $\gamma_{ss'}$.

Having considered a lens with virtually no variation of distortion, we now turn to an example of a lens which exhibits moderate distortion variation with focused distance, but only a small variation within the photographic field. The lens considered is a Schneider Super-Symmar HM MC 120-mm, *f*/5.6 lens (hereafter referred to simply as S120) which is one of the two standard lenses provided with the CRC-2 medium format camera from GSI. Throughout the focusing range of 10× to 20×, the distortion behavior of the S120 is exemplified by the profiles shown in Figure 1, which were obtained employing plumbline calibrations.

With S120 there is a very small variation of distortion within the photographic field, a fact which is again at odds with what would be anticipated from Equation 1. At a radial distance of 60mm (the working format of the CRC-2 is close to 110 by 110 mm), a difference in distortion of around 20 to 25 micrometres between the 10× and 20× values is typical. Yet the variation in distortion between image scales of 10×, 16×, and 20× for a lens focused at 13× has yet to exceed 5 micrometres at the edge of the format in the half dozen S120 lenses tested to date. For radial distances of 50 mm or less, i.e., for the main working portion of the image, the corresponding maximum value so far encountered is 2 micrometres, which is hardly significant from a practical point of view.

The next lens considered exhibits significantly larger gradients of radial distortion both with focused distance and within the photographic field. Figure 2 shows a plot of the radial distortion profiles for four focused distances and three object planes for a Nikkor SW 120-mm f/8 lens, which will be referred to as N120. The camera in question is a large-format CRC-1. Plumbline calibrations were again employed to produce this distortion data. The RMS closure of image coordinates for all profile determinations was 0.9 micrometres or less for the 900 to 1200 observations per two-photo calibration set.

The solid lines in Figure 2 show the Gaussian distortion curves for four focused distances, namely image scales of 8×, 12×, 16×, and 20×. The behavior exhibited is consistent to an accuracy of a few micrometres with that modeled by the formula given by Brown (1971, 1972):

$$\delta r_s = \alpha_s \, \delta r_{s_1} + (1 - \alpha_s) \, \delta r_{s_2} \tag{3}$$

where

$$\alpha_s = \frac{s_2 - s}{s_2 - s_1} \cdot \frac{s_1 - f}{s - f} \tag{4}$$

Here δr_s, δr_{s1}, and δr_{s2} denote the radial distortion at focused distances of s, s_1, and s_2.

The dashed curves in Figure 2 show the distortion at object distances corresponding to 8×, 16×, and 20× for the N120 focussed at 12×. Here, the gradient of distortion within the photographic field is quite significant, as can be seen, for example, by the 70-micrometre variation between the values for 8× and 20× at a radial distance of 100 mm. From Equation 2, $\gamma_{ss'}$ factors of 1.04, 0.98, and 0.97, respectively, are obtained for the 8×, 16×, and 20× image scales. Yet, Equation 1 clearly does not account for the variability of distortion within the photographic field. First, a simple proportionality factor cannot produce changes in algebraic sign for different sections of a distortion curve, for example, those for the image scale of 16×. Second, even if the sign problem is ignored the magnitudes of the ratios between the distortion curves indicate that a simple constant of proportionality is not appropriate and that the correction using

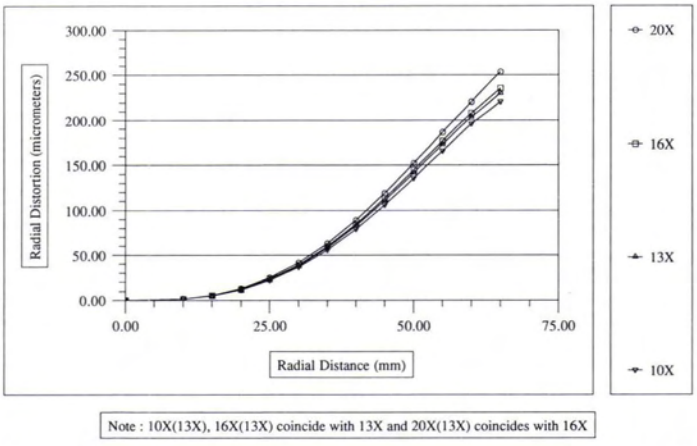

FIG. 1. Radial distortion profiles for the Schneider 120-mm lens (S120) for focused distances 10×, 13×, 16×, and 20×, and for object distances corresponding to 10×, 16×, and 20× for a focused distance of 13×. *i*×(*j*×) indicates object plane at *i*× for lens focused at *j*×.

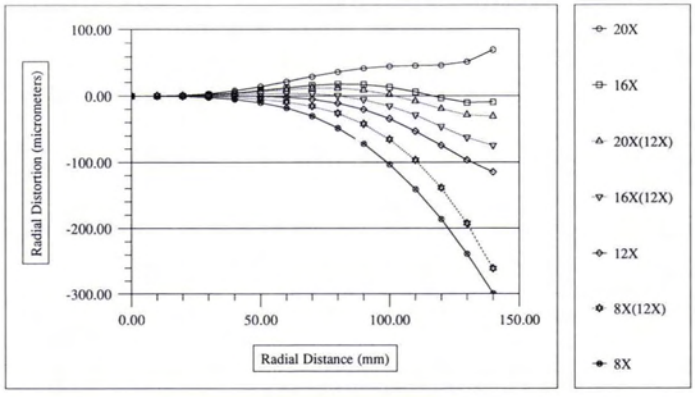

FIG. 2. Radial distortion profiles for the Nikkor 120-mm lens (N120) for focused distances 8×, 12×, 16×, and 20×, and for object distances corresponding to 8×, 16×, and 20× for a focused distance of 12×. *i*×(*j*×) indicates object plane at *i*× for lens focused at *j*×.

Equation 1 is far too conservative in any case. Third, the distortion curves for the image scale of 20× are completely reversed because, according to Equation 1, the distortions for the 12× focus should be greater than for the 20× focus.

The factor $\gamma_{ss'}$ is expressed purely as a function of $\delta r_{s'}$, yet Figure 1 suggests that both δr_s and $\delta r_{s'}$ need to be considered in any correction expression for the variation of radial lens distortion within the photographic field. Further support for this assertion is provided by the distortion characteristics of the final two lens examples, a Schneider Super-Angulon MC 65-mm *f*/5.6 lens (S65), and a Rodenstock 240-mm *f*/5.6 lens (R240). The S65 provides the wide-angle lens for the CRC-2 while the R240 forms the medium-angle option with the CRC-1.

In Figure 3, distortion plots for focused distances of 8×, 12×, 16×, and 20× are shown for S65, along with the distortion at planes 8×, 16×, and 20× for the lens focussed at 12×. In Figure 4, corresponding data are shown for R240, with the distinction that in this case the four image scales are 10×, 13×, 16×, and 20×. The profiles shown were again obtained in plumbline calibrations, the RMS closure of image coordinates being less than a micrometre for all distortion determinations.

As with the distortion profiles shown for the first three lenses, those for the S65 and R240 exhibit a distortion variation within the photographic field which is not consistent with the behavior anticipated by Equation 1. For the lenses S65, N120, and R240, however, there is one characteristic relating to the relative positions of the distortion curves at different image scales which is of practical significance. The distortion values for the object plane at $i\times$ with the lens focused at $j\times$ fall between the corresponding values for focused distances of $i\times$ and $j\times$, regardless of the algebraic sign of the $\gamma_{ss'}$ proportionality factor. This characteristic, which is also exhibited by the S120 but largely obscured by the very small variation of distortion within the photographic field, suggests that an appropriate correction function might take the following form:

$$\delta r_{ss'} = \delta r_s + F\{\delta r_{s'} - \delta r_s\}. \quad (5)$$

In the next section we will examine the effectiveness of a simple empirical expression for the function F.

AN EMPIRICAL EXPRESSION FOR $\delta r_{ss'}$

One feature exhibited in the plots of Figures 2 to 4 is that the value of the distortion difference $\delta r_{ss'} - \delta r_s$ is proportional to $\delta r_{ss'} - \delta r_{s'}$. This proportionality also appears to be reasonably linear over the full radial distance range. If the linearity were to hold true, then the function F could be replaced by a simple correction factor such that Equation 5 would take the form:

$$\delta r_{ss'} = \delta r_s + g_{ss'}(\delta r_{s'} - \delta r_s) \quad (6)$$

where $\delta r_{ss'}$ = radial distortion at an object distance s' for the lens focused at distance s, δr_s = radial distortion at an object distance s for the lens focused at distance s, $\delta r_{s'}$ = radial distortion at an object distance s' for the lens focused at distance s', and $g_{ss'}$ = a constant correction factor applicable to the lens.

We will now evaluate the validity of Equation 6 by looking at the values of $g_{ss'}$, which apply to the distortion data in Figures 2 to 4.

A simple rearrangement of Equation 6 leads to an expression for $g_{ss'}$ as a function of $dr_{ss'}$, $dr_{s'}$, and dr_s. Figure 5 shows the values of this factor for the three object planes on which the lens was not focused, for both the N120 and R240 lenses. For each lens the variability in the values of $g_{ss'}$ for different object distances is relatively small, and there is no apparent systematic change with radial distance. Between the 120-mm and 240-mm lenses, however, there is a distinct change in the $g_{ss'}$ values. Whereas a representative value for the wide-angle lens would be around 0.45, the corresponding figure for the medium-angle lens is closer to 0.25. It is tempting to suggest that this variation might be inversely proportional to lens focal length, but the data for S65 and S120 contradict this notion. With S65, experimental values for $g_{ss'}$ generally average about 0.45, though they can fluctuate substantially, as will be seen shortly. S120, on the

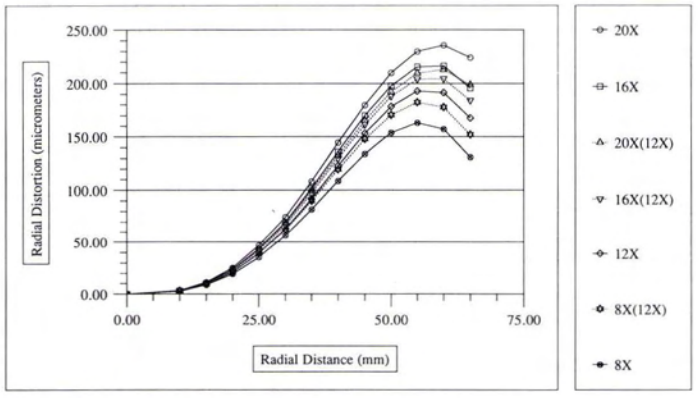

FIG. 3. Radial distortion profiles for the Schneider 65-mm lens (S65) for focused distances 8×, 12×, 16×, and 20×, and for object distances corresponding to 8×, 16×, and 20× for a focused distance of 12×. $i\times(j\times)$ indicates object plane at $i\times$ for lens focused at $j\times$.

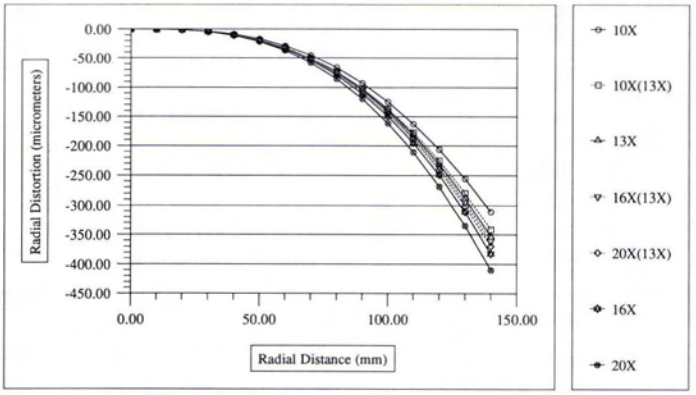

FIG. 4. Radial distortion profiles for the Rodenstock 240-mm lens (R240) for focused distances 10×, 13×, 16×, and 20×, and for object distances corresponding to 10×, 16×, and 20× for a focused distance of 13×. $i\times(j\times)$ indicates object plane at $i\times$ for lens focused at $j\times$

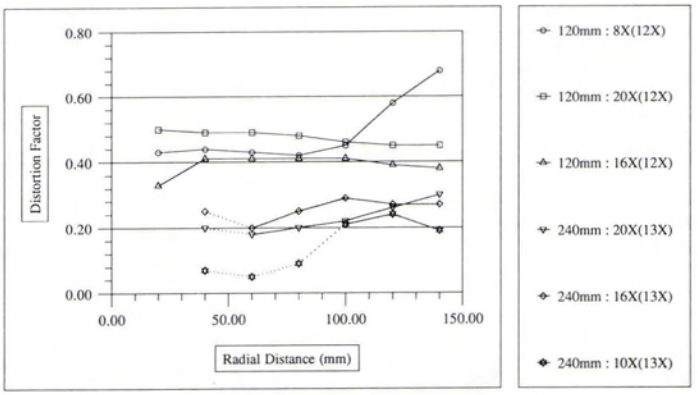

FIG. 5. Plots of the distortion factor $g_{ss'}$ against radial distance for N120 and R240 lenses. Dashed portions of the graphs indicate weak determination due to very small variation of distortion (<0.5 micrometres).

other hand, displays such a small variation of distortion within the photographic field that values of 0.1 and less for $g_{ss'}$ are typically encountered. To date, the authors have not been successful in describing the behavior of the $g_{ss'}$ factor in terms of any of the traditional photogrammetric parameters.

The plots of $g_{ss'}$ values in Figure 5 are for a single focused distance for each of the lenses. But the question of a variability in value with image scale also arises. Once again, we shall look at some experimental results to evaluate this possibility. In Figure 6, plots of $g_{ss'}$ against radial distance are shown for different object planes at three focused distances for the 120-mm lens. As in the previous figure, we again see no distinct variation in value with radial distance, but perhaps more importantly there is only limited variation with changing focused distance. These two facts have considerable practical consequence for they imply that a single value of $g_{ss'}$ might well be satisfactory to account for the variation of radial distortion within the photographic field for a given lens.

For N120 and R240 we noted that the value of $g_{ss'}$ did not display significant variation with radial distance. Such a variation is, however, exhibited by S65 at larger image scales, as is shown in Figure 7 which depicts the $g_{ss'}$ values for three different lenses at three distinct object planes for a focus of 12×. Application of a single correction factor for S65, based on a value say of 0.45, has the potential of overcorrecting radial distances where the computed $g_{ss'}$ magnitude is much smaller. While this is the case, there are two circumstances which tend to mitigate this problem in practice: first, in areas where the overcorrection is most pronounced, i.e., at small radial distances in the image, the variation of distortion within the photographic field is the least, as is clearly seen in Figure 3. Thus, application of Equation 6 generally gives rise to errors of no practical consequence. Second, the gss' curves in Figure 7 which display the steepest gradients are for image scales of 8× and 16×. These correspond to object distances of 0.6 m and 1.1 m, respectively, which are certainly shorter than the norm in everyday high-precision close-range photogrammetry.

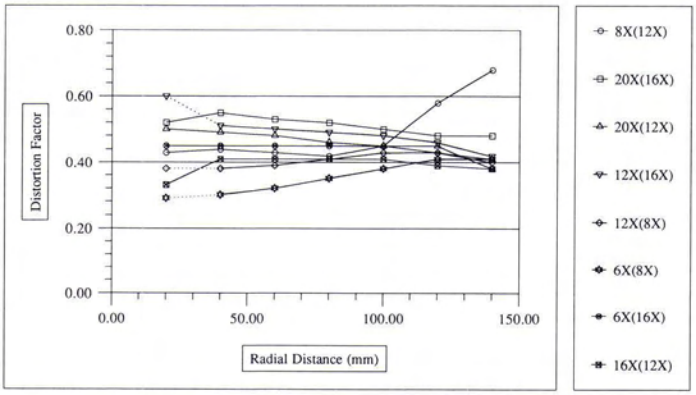

FIG. 6. Plots of the distortion factor $g_{ss'}$ against radial distance for the N120 lens at three focused distances: 8×, 12×, and 16×. Dashed portions of the graphs indicate weak determination due to very small variation of distortion (<0.5 micrometres).

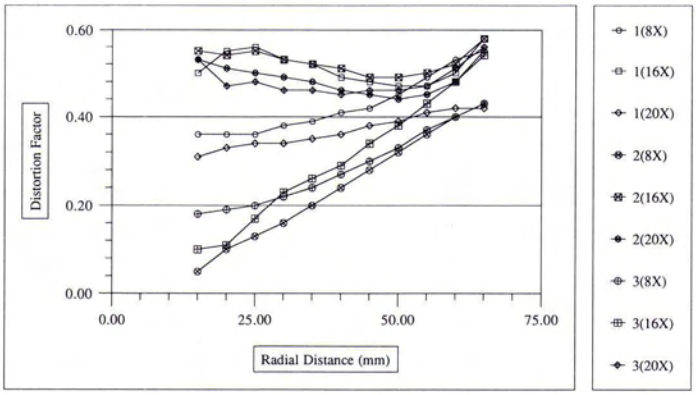

FIG. 7. Plots of the distortion factor $g_{ss'}$ against radial distance for three S65 lenses. Curves are for object planes at 8×, 16×, and 20× with the lens focused at 12×.

EXPERIMENTAL VERIFICATION OF $g_{ss'}$

In examining distortion variation it would be beneficial to create a plot equivalent to Figure 6 for each lens, and perhaps even extend it to additional focused distances. Such a proposition, however, tends to lose its appeal when it is recalled that 24 photographs and in excess of 12,000 image coordinate observations are employed to generate the nine profiles shown in the figure.

The question of the behavior of $g_{ss'}$ must still be investigated if we are to draw conclusions about the general applicability of Equation 6 as an appropriate correction formula. Thus, we now examine the results of the computation of $g_{ss'}$ factors for an additional eight Nikkor and eight Rodenstock lenses, utilizing the CRC-1 camera. These results are summarized in Tables 2 and 3 for the wide- and medium-angle lenses, respectively.

TABLE 2. RESULTS OF $g_{ss'}$ DETERMINATIONS FOR EIGHT NIKKOR 120-MM *f*/8 LENSES (N120) FITTED INTO CRC-1 CAMERAS. LENS FOCUSED AT 12×. OVERALL MEAN VALUE FOR $g_{ss'}$ IS 0.44 WITH A PRECISION OF 0.02.

Lens	$g_{ss'}$ at different object planes				Precision (one sigma) of each $g_{ss'}$ determination			RMS distortion error from application of Equation 6 with the mean $g_{ss'}$ value (micrometres)		
#	8×	16×	20×	Mean	$s_{8\times}$	$s_{16\times}$	$s_{20\times}$	$e_{8\times}$	$e_{16\times}$	$e_{20\times}$
1	0.46	0.43	0.41	0.44	0.02	0.01	0.03	2.9	<1.0	<1.0
2	0.40	0.42	0.34	0.39	0.03	0.02	0.05	2.1	1.7	<1.0
3	0.45	0.45	0.44	0.44	0.01	0.02	0.01	<1.0	<1.0	1.3
4	0.39	0.44	0.48	0.44	0.04	0.02	0.01	1.2	<1.0	1.9
5	0.44	0.40	0.51	0.45	0.03	0.01	0.04	1.8	1.4	2.1
6	0.50	0.44	0.47	0.47	0.02	0.01	0.02	1.7	1.2	<1.0
7	0.44	0.44	0.43	0.44	0.03	0.02	0.01	1.5	<1.0	<1.0
8	0.48	0.40	0.45	0.45	0.02	0.02	0.02	2.2	1.1	1.9

TABLE 3. RESULTS OF $g_{ss'}$ DETERMINATIONS FOR EIGHT RODENSTOCK 240-MM *f*/5.6 LENSES (R240) FITTED INTO CRC-1 CAMERAS. LENS FOCUSED AT 13×. OVERALL MEAN VALUE FOR $g_{ss'}$ IS 0.31 WITH A PRECISION OF 0.04.

Lens	$g_{ss'}$ at different object planes				Precision (one sigma of each) $g_{ss'}$ determination			RMS distortion error from application of Equation 6 with the mean $g_{ss'}$ value (micrometres)		
#	10×	16×	20×	Mean	$s_{10\times}$	$s_{16\times}$	$s_{20\times}$	$e_{10\times}$	$e_{16\times}$	$e_{20\times}$
1	0.30	0.30	0.43	0.34	0.03	0.03	0.06	<1.0	<1.0	1.6
2	0.32	0.36	0.39	0.36	0.04	0.05	0.04	<1.0	1.0	1.4
3	0.18	0.44	0.33	0.32	0.08	0.04	0.02	1.6	1.6	<1.0
4	0.32	0.34	0.29	0.31	0.03	0.03	0.04	<1.0	<1.0	1.7
5	0.33	0.21	0.33	0.29	0.04	0.08	0.06	1.8	<1.0	1.2
6	0.33	0.13	0.31	0.25	0.03	0.06	0.01	1.6	1.4	1.2
7	0.15	0.29	0.32	0.26	0.08	0.05	0.02	1.2	1.4	2.1
8	0.21	0.32	0.48	0.34	0.06	0.03	0.07	1.6	<1.0	2.7

In each table values of $g_{ss'}$ for three object planes are listed, along with their standard errors. These estimated values were obtained as the mean over the radial distance range of 20 to 140 mm. Also listed is the mean $g_{ss'}$ value obtained over the three image scales and the RMS error in the distortion correction which results from applying Equation 6 with this value for each lens. An overall mean value and standard deviation are additionally given for each group of eight lenses.

As can be seen in Tables 2 and 3, there is a considerable variability in the value of $g_{ss'}$ both between different object planes and between different lenses of the same type. Notwithstanding these differences, the resultant error arising from the application of Equation 6 is quite tolerable from a practical point of view. In numerous instances RMS error values of less than a micrometre result over the working image format of the camera, and in no case does the RMS error for a particular lens and object distance exceed three micrometres. Moreover, not shown in the table is the fact that the error in the computed distortion correction grows markedly at the extremities of the image format. For image points at radial distances of 100 mm or less, the individual error value rarely exceeded one micrometre. These results are moderately impressive given the magnitude of the variation of distortion within the photographic field for the N120 and R240 lenses considered.

Experimental results obtained for the Schneider 65-mm lens are very consistent with those presented in Tables 2 and 3: application of the distortion correction equation, Equation 6, yields RMS errors of less than 2 micrometres. For S65, the overall mean value of $g_{ss'}$ obtained from the five lenses tested has been found to be close to 0.45.

As has been exemplified by the case of S120, some lenses can display a variation of distortion of such a small magnitude that computation and application of the $g_{ss'}$ factor correction is not warranted for routine work. For the five Schneider 120-mm lenses tested, the correction factor averaged 0.08 and the correction yielded from Equation 6 very rarely exceeded 1 micrometre. The distortion characteristic of the S120 make it an ideal lens for high precision photogrammetric applications. Indeed, this lens, when incorporated in the CRC-2 and utilized in conjunction with AutoSet, routinely yields triangulation closures of 0.5 micrometres or less in strong multi-station close-range networks.

CONCLUDING REMARKS

In applications of close-range photogrammetry which employ medium- and large-format cameras, account must be taken of the variation of radial distortion if optimum accuracies are to be achieved. The correction of distortion variation is especially relevant to cameras using lenses with high distortion gradients, which are likely to have the largest variability. The CRC-1 and CRC-2 cameras, and the current generation of focusable semimetric cameras similar to the Pentax, clearly fall into this category as most use lenses which are not specifically designed for low distortion. Here, we have presented results which indicate that the simple empirical correction factor $g_{ss'}$ introduced in Equation 6 provides a practical and sufficiently accurate means to model the variation of distortion within the photographic field. Employment of Equation 6 overcomes the highlighted deficiencies of the correction expression, Equation 1, and in the sample data reported distortion variations of tens of micrometres were modeled by the proposed empirical correction formula to accuracies of a micrometre or two.

Routine application of the empirical correction approach necessitates, of course, the determination of the factor $g_{ss'}$, and also requires that the change of radial distortion with focused distance be known for the lens in question. At GSI these parameters are determined using an extensive plumbline calibration sequence for each CRC-1 and CRC-2 cameras produced. Indeed, the data provided for each lens in Tables 2 and 3 are taken from standard CRC-1 calibration surveys. From experience gained in numerous high precision photogrammetric measurement tasks, it has been found that object point accuracies of better than 1:250,000 and triangulation misclosures of less than one micrometre require that correction for the variability of radial distortion within the photographic field be made where warranted within the bundle adjustment.

Analytical plumbline calibration yields parameters of both radial and decentering distortion. Hence, in carrying out the work reported it was also possible to look at the variability of decentering distortion within the photographic field. For the two medium- and two large-format lenses considered there was evidence of such a distortion variation but the magnitude was on the order of only a few micrometres at most. An appropriate $g_{ss'}$ factor would be only weakly determined from such data and from a practical standpoint a correction for this level of variability is not warranted.

REFERENCES

Brown, D. C., 1971. Close-range camera calibration, *Photogrammetric Engineering*, Vol. 37, No. 8, pp. 855-866.

———, 1972. Calibration of close-range cameras, Unbound paper, Commission 5, *12th Congress of the International Society for Photogrammetry*, Ottawa, Ontario, 26 pages.

Fraser, C. S., and D. C. Brown, 1986. Industrial photogrammetry : New developments and recent applications, *Photogrammetric Record*, Vol. 12, No. 68, pp. 197-217.

Fryer, J. G., and D. C. Brown, 1986. Lens distortion for close-range photogrammetry, *Photogrammetric Engineering & Remote Sensing*, Vol. 52. No. 1, pp. 51-58.

(Received 14 June 1991; accepted 1 October 1991)